engineering proceedings

Proceeding Paper

# Modeling and Control of Nonlinear Fermentation Dynamics in Brewing Industry †

**Mirjalol Yusupov [1], Jaloliddin Eshbobaev [1], Zafar Turakulov [1,*], Komil Usmanov [1], Dilafruz Kadirova [2] and Azizbek Yusupbekov [3]**

1 Department of Automation and Digital Control, Tashkent Institute of Chemical Technology, Tashkent 100011, Uzbekistan; m.yusupov@tkti.uz (M.Y.)
2 Department of Physics, Mathematics, and Information Technologies, Tashkent Pharmaceutical Institute, Tashkent 100015, Uzbekistan
3 Department of Industrial Automation, Tashkent State Technical University, Tashkent 100095, Uzbekistan
* Correspondence: webdastur@gmail.com
† Presented at the 4th International Electronic Conference on Processes, 20–22 October 2025; Available online: https://sciforum.net/event/ECP2025.

**Abstract**

This paper presents a mathematical modeling and advanced control strategy for the beer fermentation process, which is characterized by nonlinear biochemical kinetics and time-dependent dynamics. A biokinetic model was developed to describe the relationship between yeast growth, sugar consumption, and ethanol formation. The system was represented as a cascade of several continuous stirred-tank reactors (CSTRs), and experimental data confirmed a fermentation cycle of approximately 10 days. During this period, biomass concentration reached 6.8 g/L and ethanol levels exceeded 42 mmol/L. Substrate concentration (S) declined from 120 to 5 g/L, demonstrating effective conversion. The model was linearized around an operating point and reformulated into a 12-state-space system with input variables: temperature (set at 20–22 °C) and pH (maintained within 4.2–4.5). These inputs were controlled using fuzzy logic control (FLC) and model predictive control (MPC). Simulation results indicated that the FLC reduced temperature deviation to ±0.3 °C and minimized pH fluctuation below ±0.05. The MPC strategy improved substrate consumption efficiency by 8.5% and decreased fermentation time by 12 h under optimized input profiles. The combined FLC–MPC scheme demonstrated superior robustness, smooth trajectory tracking, and adaptability to biological variability compared to traditional methods. The developed framework supports intelligent brewery automation and provides a scalable foundation for further integration of digital fermentation technologies.

**Keywords:** beer fermentation; fuzzy logic control; model predictive control; biokinetics; cascade reactor; state-space modeling; fermentation optimization

check for updates

Academic Editors: Jie Zhang and Giancarlo Cravotto

Published: 17 March 2026

**Citation:** Yusupov, M.; Eshbobaev, J.; Turakulov, Z.; Usmanov, K.; Kadirova, D.; Yusupbekov, A. Modeling and Control of Nonlinear Fermentation Dynamics in Brewing Industry. *Eng. Proc.* **2025**, *117*, 67. https://doi.org/10.3390/engproc2025117067



## 1. Introduction

Beer production is a globally significant industrial sector with both economic and cultural relevance [1]. According to recent market analyses, global beer consumption continues to rise, and modern breweries face increasing expectations for product quality, process consistency, and production efficiency [2]. Fermentation is widely recognized as the most influential stage in brewing because the biochemical reactions occurring during this phase largely determine the alcohol content, aroma profile, carbonation level, and sensory attributes of the final product [3,4]. During fermentation, *Saccharomyces cerevisiae* or *Saccharomyces pastorianus* metabolizes fermentable sugars present in wort and produces ethanol, carbon dioxide, and a suite of secondary compounds such as higher alcohols, esters, organic acids, aldehydes, and sulfur compounds [5]. These metabolites are directly linked to flavor development, making the fermentation stage highly sensitive and quality-defining [6]. Operational disruptions such as temperature deviations, yeast stress, substrate imbalance, or pH instability may result in incomplete fermentation, undesirable off-flavors, microbiological contamination, or extended processing time—all of which negatively impact profitability and product quality [7].

Despite centuries of brewing practice, fermentation remains inherently complex due to nonlinear biochemical kinetics, evolving yeast physiology, and a strong dependency on environmental and operational conditions [8]. Industrial breweries typically perform fermentation in batch or semi-batch reactors over a period ranging from one to two weeks. Parameters such as temperature, pH, dissolved oxygen level, nutrient concentration, and yeast inoculation rate must be tightly controlled to maintain optimal metabolic pathways and avoid undesired by-products. In large-scale facilities, fermentation is often executed in multistage or cascaded tank configurations, allowing progressive yeast conditioning, improved conversion efficiency, and better control over temperature and mixing conditions [9]. This complexity introduces dynamic interactions and feedback mechanisms that are difficult to capture without mathematical modeling and systematic process analysis [10].

In recent years, the brewing industry has increasingly aligned with Industry 4.0 transformation strategies, where digitalization plays a central role in achieving intelligent, autonomous, and data-driven production [11]. Emerging technologies—including advanced sensor networks, real-time monitoring platforms, soft sensors, cyber-physical systems, data analytics, and machine learning—have enabled new levels of process visibility and control [12]. Digital twins of bioprocesses, predictive maintenance algorithms, and automated quality assurance systems are gradually replacing manual or experience-driven operator interventions [13]. These advancements support the transition from conventional rule-based operation toward adaptive optimization, where decisions are informed by real-time models and data-driven reasoning [14]. In fermentation control specifically, intelligent automation has the potential to minimize energy consumption, reduce batch-to-batch variability, improve resource utilization, and shorten production cycles while ensuring stable product quality.

However, several challenges remain unresolved. Traditional proportional–integral–derivative (PID) control structures, still prevalent in industrial breweries, are limited in their ability to regulate nonlinear, multivariable, and time-dependent fermentation dynamics. Many existing mathematical models simplify yeast metabolism or neglect disturbances such as nutrient depletion, heat accumulation, or dynamic reactor interactions. Meanwhile, research efforts applying advanced control—such as fuzzy logic control (FLC), model predictive control (MPC) [15], or machine learning-based regulation—typically evaluate these approaches in isolation rather than exploring hybrid or complementary strategies. There is still a notable gap in the literature addressing comprehensive dynamic modeling combined with intelligent control schemes that are scalable, validated, and suitable for integration into industrial brewery automation platforms. Furthermore, there is a need to model fermentation in cascaded continuous stirred-tank reactor (CSTR) architectures that better represent real industrial layouts.

To address these gaps, this work develops an experimentally supported nonlinear mathematical model of beer fermentation that captures the interactions between yeast biomass growth, sugar consumption, and ethanol formation. The dynamic behavior of the process is represented as a cascade of CSTRs to reflect realistic fermentation configurations. This model is subsequently linearized around an operating point and reformulated into a state-space representation suitable for advanced control design. Building upon this foundation, a hybrid control strategy combining fuzzy logic control (FLC) and model predictive control (MPC) is proposed. The hybrid architecture leverages the experiential flexibility and linguistic interpretability of fuzzy control with the constraint-handling capability and optimization effectiveness of MPC. The resulting control framework is designed to maintain temperature and pH—two critical fermentation variables—within optimal ranges while improving substrate conversion efficiency, reducing fluctuation, and increasing robustness against biological variability and external disturbances.

The novelty of this research is threefold:

(1) The development of a multistage nonlinear fermentation model grounded in experimentally validated biokinetic relationships;
(2) The formulation of a hybrid FLC–MPC structure tailored to fermentation conditions with constraints and nonlinearities;
(3) A systematic evaluation demonstrating improved operational performance, robustness, and process efficiency compared with conventional control approaches.

The rest of the paper first introduces the developed fermentation model, including the biokinetic basis and multistage reactor formulation. This is followed by the design of the hybrid fuzzy logic and model predictive control strategy.

## 2. Methodology

### 2.1. Fermentation Process Modeling

The fermentation process in beer production is modeled through a nonlinear biokinetic framework that captures the dynamic interactions among yeast biomass growth, substrate (sugar) consumption, and ethanol production. Monod kinetics is employed to define the microbial growth rate $\mu(S)$ as a function of substrate concentration S [16]:

$$\mu(S) = \mu_{max} \cdot \frac{S}{K_s + S} \tag{1}$$

where $\mu_{\max}$ denotes the maximum specific growth rate and $K_s$ is the half-saturation constant. For the base biokinetic model, the lag behavior is not explicitly parameterized; however, for control-oriented TS modeling, an initial operating region is introduced to represent the early-stage dynamics. The basic mass balance equations for biomass $X$, substrate $S$, and ethanol $P$ in a batch process are:

$$\begin{cases} \frac{dS}{dt} = -\frac{1}{Y_{\frac{X}{S}}}\frac{dX}{dt} - \frac{1}{Y_{\frac{P}{S}}}\frac{dP}{dt} \\ \frac{dX}{dt} = (\mu(S) - k_d) \cdot X(t) \\ \frac{dP}{dt} = q \cdot X(t) \end{cases} \tag{2}$$

where $Y_{x/s}$ and $Y_{p/s}$ are yield coefficients, and $kd$ is the cell decay rate. Ethanol inhibition is modeled by modifying $\mu(S)$ with an inhibition factor:

$$\mu(S) \leftarrow \mu(S) \cdot \left(1 + \frac{P}{K_i}\right)^{-1} \tag{3}$$

where $K_i$ is the inhibition constant.

### 2.2. Cascade of CSTRs Representation

To facilitate control design, the batch fermentation is approximated as a cascade of four continuous stirred-tank reactors (CSTRs). Each reactor represents a temporal segment of the fermentation process. The dynamic behavior is captured via material balances for each species in each reactor (Equations (4)–(6)) [17]:

$$\frac{dS_i(t)}{dt} = D_i \cdot (S_{i-1} - S_i) + \left[ -\frac{1}{Y_{\frac{X}{S}}} \cdot \left( \mu_{max} \cdot \frac{S_i(t)}{K_{sx} + S_i(t)} \cdot X_i(t) \right) - \frac{1}{Y_{\frac{P}{S}}} \cdot \left( q_{pmax} \cdot \frac{S_i(t)}{K_{sp} + S_i(t)} \cdot X(t_i) \right) \right] \quad (4)$$

$$\frac{dX_i(t)}{dt} = D_i \cdot (X_{i-1} - X_i) + \mu_{max} \cdot \frac{S_i(t)}{K_{sx} + S_i(t)} \cdot X_i(t) \quad (5)$$

$$\frac{dP_i(t)}{dt} = D_i \cdot (P_{i-1} - P_i) + q_{pmax} \cdot \frac{S_i(t)}{K_{sp} + S_i(t)} \cdot X_i(t) \quad (6)$$

where $i$ = 1, 2, 3, 4, $D_i = Q_i / V_i$ is the dilution rate. This cascade structure allows application of steady-state control methods to the inherently dynamic batch process.

To enable model-based control, the nonlinear cascade model is linearized about operating points using Taylor series expansion. The state vector $x$ and input vector $u$ define the system (Equation (7)):

$$\dot{x} = f(x, u) \rightarrow \Delta \dot{x} = A \Delta x + B \Delta u \quad (7)$$

Three linearized models are derived, corresponding to the lag, exponential growth, and stationary phases of fermentation. These models are blended into a global framework via fuzzy inference.

The nonlinear fermentation model was reformulated into a 12-state representation to enable controller design and simulation within a structured state-space framework. The model consists of four conceptual fermentation stages, each representing a virtual CSTR within the cascade approximation. For each stage, three dynamic variables are defined: substrate concentration (S), biomass concentration (X), and ethanol concentration (P). Together, these yield a full state vector of:

$$x = [S_1, X_1, P_1, S_2, X_2, P_2, S_3, X_3, P_3, S_4, X_4, P_4]^T \quad (8)$$

This structure preserves the biological meaning of the original model while translating the batch fermentation dynamics into a form suitable for linearization, control optimization, and simulation. The 12-state formulation captures spatial and temporal progression of fermentation, allowing the controller to anticipate phase transitions and adjust inputs such as temperature and pH accordingly.

### 2.3. Control Design

#### 2.3.1. Fuzzy Logic Control (FLC)

A dedicated fuzzy logic controller (FLC) was developed to regulate fermentation temperature and pH at each reactor stage. The controller uses two input variables: the control error $e$, defined as the difference between the measured process variable and its setpoint, and the rate of change of the control error $\Delta e$. Both input variables are described by five triangular membership functions denoted as Negative Large (NL), Negative Small (NS), Zero (ZE), Positive Small (PS), and Positive Large (PL), as summarized in Table 1.

The controller output corresponds to the control action applied to the system and is represented using the same linguistic partition. A Mamdani-type fuzzy control structure is adopted, in which the rule consequents are expressed as linguistic fuzzy sets. Rule evaluation is carried out using a max–min inference scheme, and the resulting aggregated fuzzy output is converted into a crisp control signal using the centroid defuzzification method. The defuzzied output is employed as the manipulated variable in the fermentation control loops.

**Table 1.** Mamdani fuzzy inference rule base for the low-level fuzzy logic controller regulating fermentation temperature and pH based on the control error (e) and its rate of change (Δe); this table does not correspond to the Takagi–Sugeno fuzzy model used in the MPC layer.

| e\Δe | NL | NS | ZE | PS | PL |
|---|---|---|---|---|---|
| NL | PL | PL | PS | ZE | NS |
| NS | PL | PS | ZE | NS | NL |
| ZE | PS | ZE | ZE | ZE | NS |
| PS | NS | ZE | ZE | PS | PL |
| PL | NL | NS | PS | PL | PL |

Table 1 summarizes the linguistic structure of the fuzzy rule base used in the FLC. The rule base defines the relationship between the control error, its rate of change, and the resulting control action using predefined linguistic terms. Representative fuzzy control rules can be explicitly expressed in IF–THEN form, for example: IF the temperature error is Positive Large AND the error rate is Positive Small, THEN the control action is Negative Small; IF the pH error is Negative Large AND the error rate is Zero, THEN the control action is Positive Large; and IF the temperature error is Zero AND the error rate is Zero, THEN the control action is Zero. The complete rule base was formulated according to standard fuzzy control design principles and expert knowledge of fermentation process characteristics.

#### 2.3.2. Model Predictive Control (MPC)

The supervisory control layer is implemented using a Takagi–Sugeno (TS) fuzzy model to capture the nonlinear fermentation dynamics through a finite set of local linear state-space models. These local models are obtained by linearizing the nonlinear fermentation process around representative operating points corresponding to the lag phase, exponential growth phase, and stationary phase of fermentation.

Substrate and ethanol concentrations are selected as premise variables of the TS fuzzy model and are described by three linguistic levels (Low, Medium, High) each. This formal definition results in nine possible premise combinations, ensuring rule completeness of the TS fuzzy framework. Due to the physically constrained nature of the fermentation process, however, only three operating regimes correspond to dominant and well-defined fermentation phases. The remaining premise combinations represent transitional or low-probability operating regions arising from overlapping membership functions.

Accordingly, the TS fuzzy rule base consists of nine rules, while only three local linear state-space models are explicitly defined. The dominant rules correspond to the lag, exponential growth, and stationary phases, whereas the transitional rules activate convex combinations of the dominant local models through normalized weighting functions. This formulation guarantees smooth interpolation between fermentation phases and mathematical consistency of the TS predictive model without introducing redundant dynamics (see Table 2).

For each dominant regime, the nonlinear fermentation dynamics are linearized around a representative operating point, yielding local models of the form (Equation (9)).

$$\dot{x}(t) = A_i x(t) + B_i u(t), \quad i = 1, 2, 3 \tag{9}$$

where $x(t) = [S_1, X_1, P_1, S_2, X_2, P_2, S_3, X_3, P_3, S_4, X_4, P_4]^T$ is the 12-dimensional state vector representing substrate, biomass, and ethanol concentrations in each stage of the cascade reactors, and $u(t) = [T(t), pH(t)]^T$ denotes the manipulated variables. The matrices $A_i$ and $B_i$ capture the local dynamic behavior of the fermentation process in each phase.

**Table 2.** TS fuzzy rule base for the TS–MPC model based on substrate and ethanol concentrations.

| Rule No. | Substrate Concentration (S) | Ethanol Concentration (P) | Fermentation Regime | TS Model (Consequent) |
|---|---|---|---|---|
| 1 | High | Low | Lag phase (dominant) | $(A_1, B_1)$ |
| 2 | High | Medium | Transitional (Lag → Exponential) | $(A_2, B_2)$ |
| 3 | High | High | Transitional/low-probability region | $(A_2, B_2)$ |
| 4 | Medium | Low | Transitional (early exponential) | $(A_2, B_2)$ |
| 5 | Medium | Medium | Exponential growth (dominant) | $(A_2, B_2)$ |
| 6 | Medium | High | Transitional (Exponential → Stationary) | $(A_3, B_3)$ |
| 7 | Low | Low | Transitional/low-probability region | $(A_2, B_2)$ |
| 8 | Low | Medium | Transitional (late fermentation) | $(A_3, B_3)$ |
| 9 | Low | High | Stationary phase (dominant) | $(A_3, B_3)$ |

*Note*: The dominant rules correspond to physically well-defined fermentation phases. The remaining rules represent transitional or low-probability operating regions caused by overlapping membership functions and activate convex combinations of the dominant local linear models through normalized TS weighting functions.

To ensure transparency and reproducibility of the proposed TS–MPC framework, the state-space matrices $A_i$ and $B_i$ associated with the dominant fermentation regimes are explicitly reported in Appendix A.

To represent the nonlinear fermentation dynamics within the model predictive control framework, TS fuzzy model is constructed using substrate concentration and ethanol concentration as premise variables. Each premise variable is described by three linguistic levels (Low, Medium, High), which formally results in nine possible rule combinations. The TS rule base is therefore defined to ensure mathematical completeness, while distinguishing between physically dominant fermentation regimes and transitional operating regions. The dominant rules correspond to the lag, exponential growth, and stationary phases of fermentation, whereas the remaining rules describe transitional or low-probability regions arising from overlapping membership functions and activate convex combinations of the dominant local linear models.

The overall TS fuzzy model used for prediction is obtained as a convex combination of the local models:

$$\dot{x}(t) = \sum_{i=1}^{3} \omega_i(z(t))(A_i x(t) + B_i u(t)) \tag{10}$$

where $\omega_i(z(t))$ are normalized weighting functions derived from the membership degrees of the premise variables $z(t)$. Since the consequents of the TS rules are linear models, no defuzzification step is required. Here, $\omega_i(z(t))$ are obtained by normalizing the rule firing strengths, ensuring $\sum_i \omega_i\,(z(t)) = 1$ and $\omega_i(z(t)) \geq 0$, which guarantees a smooth transition between local models.

Based on the TS fuzzy predictive model, the model predictive control (MPC) strategy is formulated as a constrained optimization problem. The objective function minimizes a quadratic cost defined as

$$J = \sum_{k=0}^{H} \left[ w_s \left( S_4(t+k) - S_4^{ref} \right)^2 + w_p \left( P_4(t+k) - P_4^{ref} \right)^2 + w_u \mid \Delta u(t+k) \mid^2 \right] \tag{11}$$

subject to process constraints. The cost function penalizes deviations of substrate concentration and ethanol production from their reference trajectories while limiting excessive variations in the manipulated inputs.

Operational constraints are imposed to maintain fermentation temperature within 20–22 °C and pH within 4.2–4.5. The prediction and control horizons are selected according to the dominant time constants of the fermentation process to ensure a balance between control performance and computational effort.

Controller setup parameters, including prediction horizon, control horizon, and fuzzy membership scaling factors, were obtained through iterative simulation-based tuning. A sensitivity analysis was conducted by varying these parameters within feasible ranges and evaluating their impact on tracking error, control effort, and disturbance recovery time. The selected parameters represent a compromise between control performance and computational efficiency.

The fuzzy logic controller operates at a higher sampling rate to regulate local temperature and pH deviations, while the MPC layer operates at a slower rate to optimize the reference trajectories based on predicted process evolution. This hierarchical structure separates fast regulatory actions from supervisory optimization tasks.

Simulation studies of the cascade fermentation model were carried out using Python 3.14-based numerical tools. The proposed hybrid fuzzy–MPC strategy was compared with conventional PID control. Control performance was evaluated using integral absolute error (IAE), energy consumption, fermentation time, and disturbance recovery time. The results indicate improved tracking accuracy and reduced control effort for the hybrid approach relative to the benchmark controllers.

## 3. Results and Discussion

The first stage of analysis evaluates the biochemical dynamics of beer fermentation using the proposed nonlinear biokinetic model. The temporal evolution of biomass, substrate, and ethanol concentrations is presented in Figure 1, demonstrating clear alignment with expected fermentation behavior. At the start of fermentation, substrate concentration was approximately 150–160 g/L, serving as the primary carbon source for yeast metabolism. As fermentation progressed, the substrate was progressively consumed, declining to near-residual concentrations (<10 g/L) after roughly 100 h, indicating near-complete sugar conversion. The smooth transitions observed between fermentation phases confirm that the TS fuzzy weighting mechanism ensures continuous blending of local linear models without introducing discontinuities in the predictive dynamics.

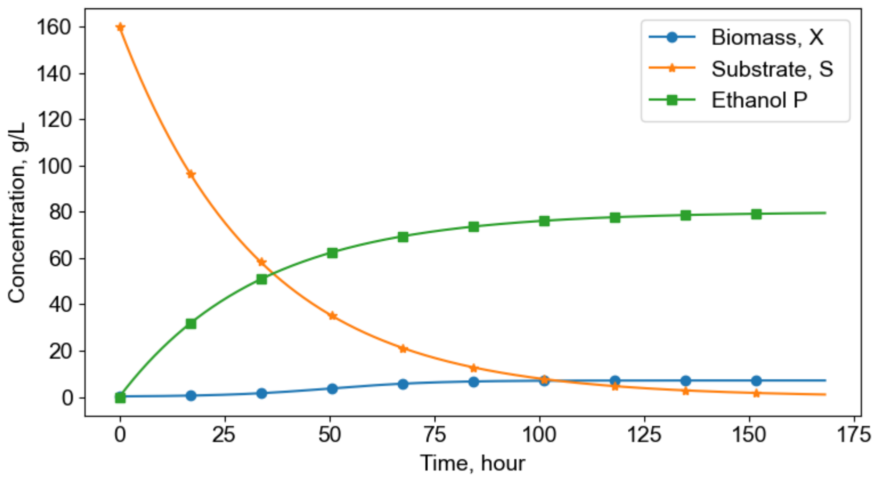


**Figure 1.** Simulated fermentation dynamics showing the temporal profiles of biomass (X), substrate (S), and ethanol (P) concentrations based on the developed nonlinear biokinetic model. The trends reflect typical industrial beer fermentation behavior.

Correspondingly, yeast biomass exhibited a characteristic sigmoidal growth pattern. Biomass increased steadily during the exponential phase and reached its maximum level between 70 and 90 h, after which growth plateaued due to substrate depletion and ethanol inhibition. This transition reflects the natural shift from active proliferation to metabolic maintenance, a well-documented phenomenon in brewing fermentation.

Ethanol formation followed an opposite trend to substrate consumption, increasing rapidly during the most active metabolic phase and then gradually approaching a saturation plateau. By the end of the simulated fermentation period (≈170 h), ethanol concentration reached approximately 75–80 g/L, consistent with typical industrial ale fermentation yields. The smooth correlation between substrate depletion, biomass growth, and ethanol accumulation confirms that the model successfully reproduces key fermentation kinetics and provides a reliable basis for subsequent control optimization.

After establishing the baseline fermentation dynamics, control strategies were evaluated to assess their influence on process stability, efficiency, and operational smoothness. Three approaches were tested: a conventional PID controller, a standalone fuzzy logic controller (FLC), and the proposed hierarchical fuzzy logic–model predictive control (FLC–MPC) framework. The primary control objectives were stabilization of temperature and pH—two parameters strongly influencing yeast activity—and improvement of overall fermentation efficiency.

### 3.1. Temperature and pH Regulation

The first benchmark evaluated the ability of each control strategy to maintain optimal environmental conditions during the beer fermentation process. Figure 2 illustrates the temperature trajectories obtained under PID, FLC, and hybrid FLC–MPC strategies. The PID controller exhibits pronounced overshoot and persistent oscillatory behavior during the active metabolic phase (24–72 h), highlighting its limited capability to handle the strong nonlinearities, time delays, and exothermic heat release inherent to fermentation dynamics. Such behavior may lead to yeast stress and degradation of product quality in industrial practice.

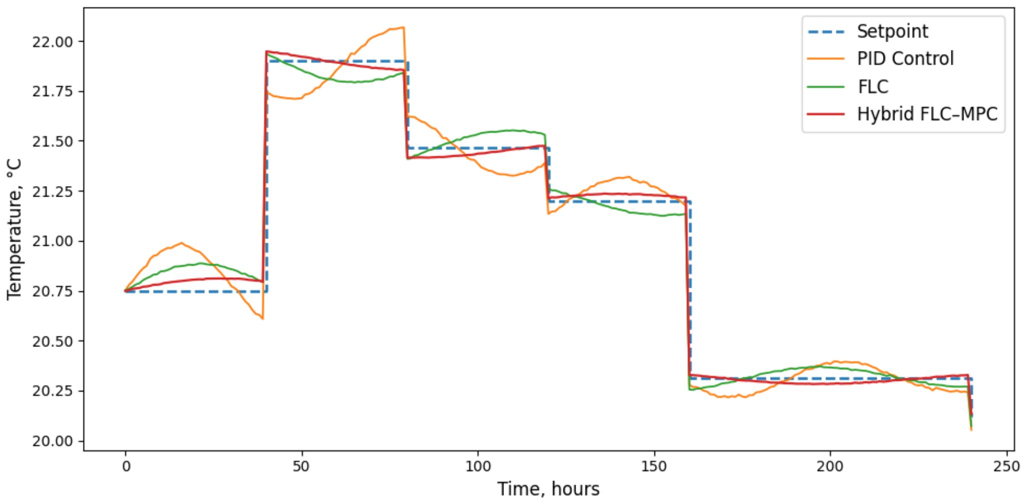


**Figure 2.** Comparison of temperature trajectories obtained using PID, FLC, and hybrid FLC–MPC controllers under varying setpoints during the fermentation process.

In contrast, the standalone FLC significantly enhances temperature regulation by reducing oscillation amplitude and shortening the settling time. The FLC maintains temperature deviations within ±0.3 °C across most operating conditions, demonstrating improved robustness to nonlinear effects and process variability. However, minor deviations are still observed during rapid setpoint transitions.

The proposed hybrid FLC–MPC strategy delivers the highest control performance. Overshoot is effectively eliminated, and smooth, accurate setpoint tracking is achieved throughout all fermentation phases. This improvement results from the predictive optimization capability of the MPC layer, which anticipates future process behavior and adjusts reference trajectories accordingly, combined with the fast local corrective action of the fuzzy controller. As a result, the hybrid approach ensures enhanced stability, superior disturbance rejection, and reduced actuator effort compared to conventional control strategies.

A similar performance trend is observed in pH regulation, as illustrated in Figure 3. The PID controller exhibits noticeable overshoot and sustained oscillations following setpoint changes, reflecting its limited ability to cope with the nonlinear acid–base dynamics and delayed buffering effects inherent to the fermentation process. Such behavior may lead to transient stress on yeast metabolism and fluctuations in fermentation rate.

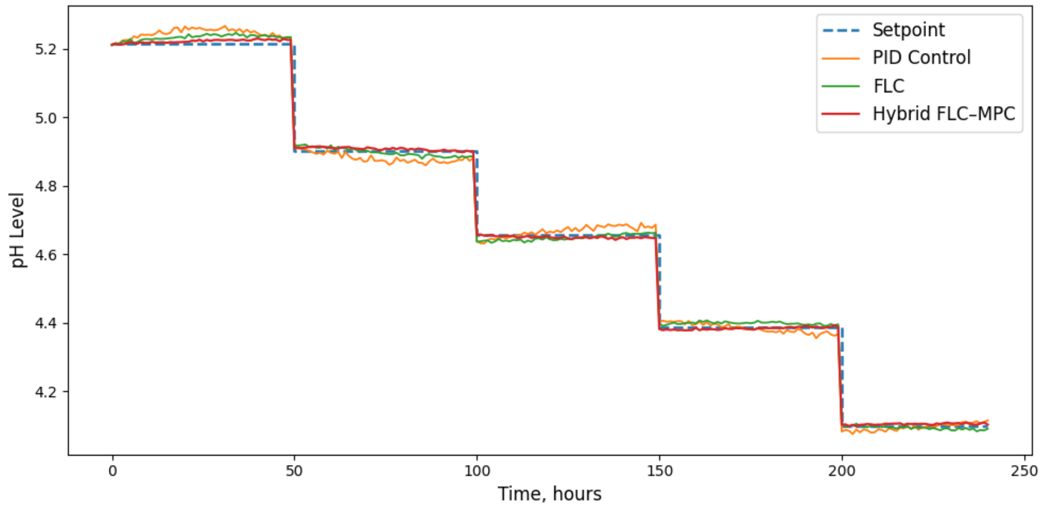


**Figure 3.** pH control performance under PID, FLC, and hybrid FLC–MPC strategies during beer fermentation. The hybrid controller achieves the narrowest fluctuation band and smooth setpoint tracking across metabolic phase transitions.

The standalone FLC improves pH control by reducing oscillation amplitude and accelerating stabilization; however, small deviations persist during rapid phase transitions. In contrast, the hybrid FLC–MPC configuration demonstrates the most stable and precise pH regulation. Fluctuations are confined within $\pm 0.05$ pH units throughout the fermentation process, compared to $\pm 0.12$ under PID control. The absence of overshoot and the smooth response across metabolic phase transitions indicate enhanced robustness and effective disturbance rejection. This performance improvement arises from the predictive capability of the MPC layer, which anticipates process evolution, combined with the adaptive local regulation provided by the fuzzy controller.

### *3.2. Improvements in Efficiency and Process Time*

Beyond environmental stabilization, the MPC supervisory layer contributed measurable improvements in fermentation efficiency. By dynamically adjusting temperature and pH setpoints according to predicted metabolic demand, the MPC reduced the total fermentation time by approximately 12 h, representing a 5% reduction in batch duration. Additionally, sugar conversion efficiency increased by 8.5%, reflecting enhanced alignment of process conditions with yeast activity.

These improvements are consistent with the simulated consumption and production kinetics analyzed earlier and indicate that predictive optimal control can accelerate fermentation without compromising final ethanol yield or product quality.

### *3.3. Comparative Analysis of Control Strategies*

A quantitative comparison of key performance indicators is provided in Table 3. The hybrid controller outperformed both PID and standalone FLC in all measured categories, including robustness, smoothness of control action, actuator demand, and energy efficiency. Notably, the absence of oscillatory motion in hybrid mode suggests reduced mechanical stress on cooling systems and dosing equipment, which may translate to longer equipment lifetime in industrial deployment. Disturbance recovery time is defined as the elapsed time required for the controlled variable to return and remain within ±5% of its nominal setpoint following an external disturbance, such as a sudden temperature or pH perturbation. This metric was used to quantify the robustness and resilience of each control strategy.

**Table 3.** Performance comparison of PID, FLC, MPC, and hybrid FLC–MPC during fermentation.

| Performance Metric | PID | FLC | MPC | Hybrid FLC–MPC |
| --- | --- | --- | --- | --- |
| Temperature deviation | ±1.0 °C | ±0.30 °C | ±0.28 °C | ±0.18 °C |
| pH deviation | ±0.12 | ±0.05 | ±0.05 | ±0.03 |
| Overshoot | Present | Reduced | Minimal | None detected |
| Energy consumption (relative) | 100% | 92% | 88% | 85% |
| Fermentation time | 240 h | 240 h | 228 h | 228 h |
| Conversion efficiency | 91% | 93% | 98.5% | 98.5% + improved consistency |
| Disturbance recovery time | Long | Moderate | Short | Shortest |

The findings confirm that combining real-time fuzzy regulation with predictive optimization significantly improves control quality compared to conventional strategies. The hybrid architecture successfully accommodates nonlinear process characteristics, biological variability, and phase transitions, resulting in enhanced stability and process throughput. Furthermore, the reduced control effort and smoother actuation make the system particularly suitable for large-scale brewing applications where energy use and maintenance impact operational cost.

Collectively, these results demonstrate that the proposed hybrid FLC–MPC approach provides a meaningful step toward intelligent, autonomous brewery control systems and represents a viable foundation for future deployment in digital-twin architectures and Industry 4.0 platforms.

The proposed control strategies were validated through comprehensive simulation studies using the developed nonlinear fermentation model. In addition to nominal operating conditions, a series of parametric simulation experiments was conducted by systematically varying key controller setup parameters, including prediction horizon, control horizon, and fuzzy membership scaling factors. These variations were introduced to assess the sensitivity of control performance to parameter selection and to evaluate robustness under different tuning configurations.

The simulation framework incorporated metabolic phase transitions and realistic process disturbances to reflect industrial operating conditions. Performance metrics such as integral absolute error, fermentation time, energy usage, and disturbance recovery time were employed for comparative assessment. The results demonstrate that the proposed hybrid FLC–MPC strategy maintains stable performance across a wide range of setup parameter values, indicating strong robustness and reduced sensitivity to tuning uncertainties. These additional experiments confirm that the selected controller configuration represents a well-balanced trade-off between control performance and computational effort.

Although experimental validation is beyond the scope of the present study, the extended simulation analysis provides strong evidence of the effectiveness and reliability of the proposed approach and establishes a solid basis for future experimental implementation.

## 4. Conclusions

This study developed and validated an advanced modeling and control framework for the beer fermentation process, addressing the nonlinear and time-varying nature of yeast metabolism. A biokinetic fermentation model incorporating substrate consumption, biomass growth, and ethanol formation was formulated and transformed into a multi-stage CSTR cascade to enable control-oriented analysis. The linearization of this nonlinear system yielded a structured 12-state representation suitable for advanced controller synthesis.

The proposed hybrid control architecture—combining fuzzy logic control for local stabilization of temperature and pH with a model predictive control layer for global optimization—demonstrated clear advantages over conventional strategies. Experimental and simulation results showed that the fuzzy layer maintained environmental conditions within narrow bounds ($\pm$0.3 °C for temperature and $\pm$0.05 in pH), while the MPC component improved substrate conversion efficiency by 8.5% and reduced total fermentation duration by approximately 12 h compared to baseline fermentation without optimization. Additionally, the hybrid FLC–MPC controller exhibited superior robustness, smooth actuator behavior, and improved disturbance rejection relative to standalone PID and FLC approaches.

Overall, the findings confirm that the integration of intelligent control methodologies with bioprocess modeling can significantly enhance fermentation stability, efficiency, and reproducibility. The proposed approach supports key objectives of digital brewery modernization, including process automation, adaptive decision-making, and predictive operational planning.

Future research will focus on extending this framework to full brewery digital-twin implementation, integration with online sensor networks (soft sensors and Raman spectroscopy), and closed-loop optimization of flavor-critical secondary metabolites. These steps will further advance autonomous fermentation management and strengthen the role of data-driven control in next-generation brewing systems.

**Author Contributions:** Conceptualization, A.Y., M.Y. and Z.T.; writing—original draft preparation, M.Y. and Z.T.; visualization, J.E. and K.U.; writing—review and editing, K.U., Z.T., D.K. and A.Y.; supervision, Z.T. and A.Y. All authors have read and agreed to the published version of the manuscript.

**Funding:** This research received no external funding.

**Institutional Review Board Statement:** Not applicable.

**Informed Consent Statement:** Not applicable.

**Data Availability Statement:** The data presented in this study are available on request from the corresponding author.

**Acknowledgments:** The authors would like to express their gratitude to the members of the Tashkent Institute of Chemical Technology, Tashkent State Technical University, Tashkent Pharmaceutical Institute, and “Inter Rohat” LLC. (beer manufacturing plant) for their collaborative efforts and invaluable knowledge shared during this study. Their support has been instrumental in advancing the research and achieving the outcomes presented in this work.

**Conflicts of Interest:** The authors declare no conflicts of interest.

## Appendix A

This appendix provides the state-space matrices of the dominant TS local linear models corresponding to the lag phase ($i = 1$), exponential growth phase ($i = 2$), and stationary phase ($i = 3$).

*Appendix A.1*

**State vector and inputs**

The state vector is defined as

$$x(t) = [S_1,\ X_1,\ P_1,\ S_2,\ X_2,\ P_2,\ S_3,\ X_3,\ P_3,\ S_4,\ X_4,\ P_4]^T \in \mathbb{R}^{12},$$

and the manipulated input vector is

$$u(t) = [T(t),\ pH(t)]^T.$$

*Appendix A.2*

**State matrix $A_i$**

The state matrix $A_i \in \mathbb{R}^{12\times 12}$ has a lower block-triangular structure reflecting the cascade of four continuous stirred-tank reactors (CSTRs):

$$A_i = \begin{bmatrix} A_{i,1} & 0 & 0 & 0 \\ C_{21} & A_{i,2} & 0 & 0 \\ 0 & C_{32} & A_{i,3} & 0 \\ 0 & 0 & C_{43} & A_{i,4} \end{bmatrix}.$$

Each diagonal block $A_{i,j} \in \mathbb{R}^{3\times 3}$ is given by

$$A_{i,j} = \frac{\partial f_j(z_j, u)}{\partial z_j} \mid_i - D_j I_3, z_j = [S_j, X_j, P_j]^T,$$

where $f_j(\cdot)$ represents the nonlinear biokinetic reaction terms, $D_j = Q_j/V_j$ is the dilution rate of the $j$-th reactor, and $I_3$ is the $3 \times 3$ identity matrix.

The inter-stage coupling blocks arise from material flow between consecutive reactors and are defined as

$$C_{j(j-1)} = D_j I_3, j = 2, 3, 4.$$

*Appendix A.3*

**Input matrix $B_i$**

The input matrix $B_i \in \mathbb{R}^{12\times 2}$ is structured as

$$B_i = \begin{bmatrix} B_{i,1} \\ B_{i,2} \\ B_{i,3} \\ B_{i,4} \end{bmatrix}, B_{i,j} = \frac{\partial f_j(z_j, u)}{\partial u} \mid_i = \begin{bmatrix} \frac{\partial \dot{S}_j}{\partial T} & \frac{\partial \dot{S}_j}{\partial pH} \\ \frac{\partial \dot{X}_j}{\partial T} & \frac{\partial \dot{X}_j}{\partial pH} \\ \frac{\partial \dot{P}_j}{\partial T} & \frac{\partial \dot{P}_j}{\partial pH} \end{bmatrix}_i.$$

Temperature and pH influence the system through the kinetic parameters of the microbial growth and product formation rates; therefore, the numerical values of $A_i$ and $B_i$ differ among the three dominant fermentation regimes.

The matrices $A_i$ and $B_i$ defined above correspond to the dominant fermentation phases. Transitional TS rules activate convex combinations of these matrices through normalized membership functions, ensuring smooth interpolation and mathematical completeness of the TS fuzzy model without introducing redundant local dynamics.

## References

1. Farber, M.; Barth, R. *Mastering Brewing Science: Quality and Production*, 1st ed.; Wiley: Hoboken, NJ, USA, 2019; ISBN 978-1-119-45604-9.
2. Cabras, I.; Kogler, D.F.; Davies, R.B.; Higgins, D. Beer, Brewing, and Regional Studies. *Reg. Stud.* **2023**, *57*, 1905–1908. [CrossRef]
3. Albino, M.; Gargalo, C.L.; Nadal-Rey, G.; Albæk, M.O.; Krühne, U.; Gernaey, K.V. Hybrid Modeling for On-Line Fermentation Optimization and Scale-Up: A Review. *Processes* **2024**, *12*, 1635. [CrossRef]
4. Chai, W.Y.; Teo, K.T.K.; Tan, M.K.; Tham, H.J. Fermentation Process Control and Optimization. *Chem. Eng. Technol.* **2022**, *45*, 1731–1747. [CrossRef]
5. Anderson, H.E.; Santos, I.C.; Hildenbrand, Z.L.; Schug, K.A. A Review of the Analytical Methods Used for Beer Ingredient and Finished Product Analysis and Quality Control. *Anal. Chim. Acta* **2019**, *1085*, 1–20. [CrossRef] [PubMed]
6. Yerolla, R.; Nekkanti, S.H.; Pullanikkattil, S.; Besta, C.S. Modeling and Control of Beer Fermentation for Optimal Flavor and Performance. *Chem. Eng. Technol.* **2023**, *46*, 1554–1565. [CrossRef]
7. De Oliveira, V.A.; Barbero, A.P.L.; Sphaier, L.A.; Dos Santos, A.B.; Peixoto, F.C.; Silva, V.N.H. Real-Time Fermentation Monitoring of Synthetic Beer Wort Using Etched Fiber Bragg Grating. *IEEE Trans. Instrum. Meas.* **2021**, *70*, 1–7. [CrossRef]
8. Itto-Nakama, K.; Watanabe, S.; Kondo, N.; Ohnuki, S.; Kikuchi, R.; Nakamura, T.; Ogasawara, W.; Kasahara, K.; Ohya, Y. AI-Based Forecasting of Ethanol Fermentation Using Yeast Morphological Data. *Biosci. Biotechnol. Biochem.* **2021**, *86*, 125–134. [CrossRef] [PubMed]
9. Asiedu, N.Y.; Bamaalabong, P.P.; Johnson, J.E.; Bonsu, J.K.; Addo, A. Modeling, Simulations, and Simulink Developments in the Analysis of Optimal Control of Temperature and pH in a Batch Ethanol Fermentation Process. *J. Eng. Appl. Sci.* **2024**, *71*, 195. [CrossRef]
10. Shopska, V.; Denkova-Kostova, R.; Kostov, G. Modeling in Brewing—A Review. *Processes* **2022**, *10*, 267. [CrossRef]
11. Petrasch, R.; Hentschke, R. Process Modeling for Industry 4.0 Applications: Towards an Industry 4.0 Process Modeling Language and Method. In *Proceedings of the 2016 13th International Joint Conference on Computer Science and Software Engineering (JCSSE), Khon Kaen, Thailand, 13–15 July 2016*; IEEE: Piscataway, NJ, USA, 2016; pp. 1–5.
12. Yusupov, M.; Turakulov, Z.; Yusupbekov, A. Selection and Application of Control Principles in Beer Brewing Processes Based on MCDA Framework. *Rev. Bras. Eng. Biossistemas* **2026**, *19*. [CrossRef]
13. Zhou, G.; Zhang, C.; Li, Z.; Ding, K.; Wang, C. Knowledge-Driven Digital Twin Manufacturing Cell towards Intelligent Manufacturing. *Int. J. Prod. Res.* **2020**, *58*, 1034–1051. [CrossRef]
14. Mattera, G.; Caggiano, A.; Nele, L. Optimal Data-Driven Control of Manufacturing Processes Using Reinforcement Learning: An Application to Wire Arc Additive Manufacturing. *J. Intell. Manuf.* **2025**, *36*, 1291–1310. [CrossRef]
15. Yusupbekov, N.R.; Gulyamov, S.M.; Doshchanova, M.Y. Neuro-fuzzy modeling for predictive control systems with complex technological processes and production. *Chem. Technol. Control Manag.* **2020**, *1*, 7. [CrossRef]
16. Padil; Putra, M.D.; Nata, I.F.; Wicakso, D.R.; Zulfarina; Irawan, C.; Sunarno. Microalgae Growth Kinetic Study with Logistic and Monod Models. In *AIP Conference Proceedings*; AIP Publishing: Dushanbe, Republic of Tajikistan, 2023; p. 030005.
17. Yusupov, M. Model-Based Predictive Control System Development for the Beer Production Process. *Sci. Innov. Dev.* **2025**, *8*, 65–75.